ARTICLE
Journal of Cellular Biochemistry 115:2022–2032 (2014)

Journal of Cellular Biochemistry

Verrucarin A Induces Apoptosis Through ROS-Mediated EGFR/MAPK/Akt Signaling Pathways in MDA-MB-231 Breast Cancer Cells

Kandasamy Palanivel,[1] Veerasamy Kanimozhi,[1] Balamuthu Kadalmani,[1]* and Mohammad Abdulkader Akbarsha[2]

[1]*Department of Animal Science, Bharathidasan University, Tiruchirappalli 620024, Tamil Nadu, India*

[2]*Mahatma Gandhi-Doerenkamp Centre (MGDC), Bharathidasan University, Tiruchirappalli 620024, Tamil Nadu, India*

ABSTRACT

The present study was carried out to elucidate the mechanisms underlying Verrucarin A (VA)-induced cytotoxicity in human breast cancer cell line MDA-MB-231. VA inhibited the growth of MDA-MB-231 cells by induction of reactive oxygen species (ROS)-dependent mitochondrial apoptosis. Elevation of ROS production, associated with changes in Bax/Bcl-2 ratio, led to loss of mitochondrial membrane potential ($\Delta\psi m$) and cytochrome *c* release in VA-treated cells. Release of cytochrome *c* from mitochondria to cytosol triggered activation of caspase-3, PARP cleavage, DNA fragmentation, and finally apoptotic cell death. Furthermore, VA-induced apoptosis was accompanied by the activation of p38MAPK and inhibition of phosphorylation of EGFR as well as of Akt and ERK1/2. However, pre-treatment with *n*-acetyl cysteine, an ROS scavenger, and SB202190, a p38MAPK inhibitor, significantly inhibited VA-induced ROS generation, EGFR inhibition, p38MAPK activation and apoptosis. Moreover, pharmacological inhibition of EGFR and ERK1/2 significantly accelerated the VA-induced apoptosis in MDA-MB-231 cells. Collectively, these results indicate that VA-induces ROS elevation in cancer cells, which results in the activation of p38MAPK and inhibition of EGFR/Akt/ERK signaling cascade and, ultimately, cancer cell death. J. Cell. Biochem. 115: 2022–2032, 2014.

KEY WORDS: APOPTOSIS; EPIDERMAL GROWTH FACTOR RECEPTOR; MAPK; REACTIVE OXYGEN SPECIES; VERRUCARIN A

Aberrations in cellular signaling pathways are commonly associated with atypical cell growth, disrupted cell cycle progression, and dysregulated apoptotic responses in cancer. The aberrations in the cellular signaling pathways are due to over-expression or loss/gain of function in growth factor receptors and/or regulatory proteins. Epidermal growth factor receptor (EGFR), a proto-oncogene that belongs to a family of transmembrane receptor tyrosine kinases (RTKs), is implicated in diverse cellular functions such as proliferation, differentiation, angiogenesis, and suppression of apoptosis. In particular, EGFR is over-expressed in a majority of triple negative breast cancers (TNBCs) as well as other cancers and portends poor prognosis, inferior survival, radioresistance, and treatment failures [Peddi et al., 2012]. EGFR is over-expressed in about 30% of breast cancers and is considered as a potential target therapeutic intervention for triple-negative breast cancers. EGF receptor undergoes dimerization following ligand binding (e.g., EGF and TGF-α) and acts as a binding site for signal transducers responsible for cell proliferation, motility and survival [Zandi et al., 2007].

Aberrant activation of EGFR relays growth signals through its various downstream signal transduction cascades, including MAPK, PI3K/AKT, and STAT3, contributing to mitogenic and prosurvival responses [Looyenga et al., 2012]. Besides, reactive oxygen species (ROS) act as major mediator of stress-induced signaling, and the elevation of cellular ROS has been connected to cellular damage in cancer [Kamata and Hirata, 1999]. Oxidative stress stimuli trigger autophosphorylation of a variety of RTKs including EGFR, which are particularly sensitive to stress-induced activation [Rao, 1996]. Inhibition of EGFR expression leads to downregulation of these signaling cascades resulting in apoptosis of cancer cells [Selvendiran

The authors declared that there are no conflicts of interest.
Grant sponsor: University Grants Commission, New Delhi, India.
*Correspondence to: Balamuthu Kadalmani, Department of Animal Science, School of Life Sciences, Bharathidasan University, Tiruchirappalli 620024, Tamil Nadu, India. E-mail: kadalmanibdu@rediffmail.com
Manuscript Received: 25 April 2014; Manuscript Accepted: 13 June 2014
Accepted manuscript online in Wiley Online Library (wileyonlinelibrary.com): 25 June 2014
DOI 10.1002/jcb.24874 • © 2014 Wiley Periodicals, Inc.

et al., 2008]. Previous studies have also shown that the mitogen-activated protein kinase (MAPK) pathways are critical for converting diverse extracellular signals, including ROS, to apoptotic responses during treatment with chemotherapeutic agents. Of these, extracellular signal-regulated kinase 1/2 (ERK1/2) acts as a mitogen-activated proliferation/differentiation factor, whereas JNK and p38MAPK are mainly stress-activated proteins related to apoptotic cell death [Tamura et al., 2002].

Verrucarin A (VA) is a class of naturally occurring macrocyclic trichothecene produced by several pathogenic fungi such as *Fusarium*, *Myrothecium verrucaria*, and *Stachybotrys* [Andersen et al., 2002]. It has been already reported that VA inhibits the growth of several cancer cell lines including renal carcinoma, hepatocellular carcinoma, leukemia, and breast carcinoma [Oda et al., 2005]. VA has been shown to activate stress responses and caspases and induce DNA damage and apoptosis through MAPK pathway. Recently, we have also demonstrated that VA-induced cytotoxicity is associated with upregulation of pro-apoptotic Bax and downregulation of anti-apoptotic Bcl-2 protein in MDA-MB-231 and T47D cells [Palanivel et al., 2013]. The aim of the present study was to investigate the molecular mechanisms underlying VA-induced cytotoxicity in human triple-negative breast cancer cell line MDA-MB-231. Our data demonstrate that VA-induced apoptosis is effected through ROS-dependent EGFR/Akt/MAPK signal transduction pathways, followed by activation of caspase-3 and PARP cleavage in MDA-MB-231 cells.

MATERIALS AND METHODS

CELL CULTURE, DRUGS, ANTIBODIES, AND REAGENTS

Breast cancer cell line MDA-MB-231 (estrogen receptor-negative, metastatic and harboring a mutant form of p53, as well as over-expression of the EGFR) was obtained from National Centre for Cell Science (NCCS, Pune, India). Cells were maintained in Dulbecco's modified Eagle's medium (DMEM) containing 10% heat-inactivated fetal bovine serum (HI-FBS; Gibco, USA) and 100 units/ml each of penicillin and streptomycin. VA (purity > 98%), JC-1 (5,5′,6,6′-tetrachloro-1,1′,3,3′-tetraethyl-benzimidazol-carbocyanine iodide) and NAC (*n*-acetyl L-cysteine) were purchased from Sigma Aldrich (St. Louis, MO). All cell culture reagents were purchased from Invitrogen (Carlsbad, CA). Primary antibodies, anti-Bax, anti-Bcl-2, anti-cytochrome *c*, anti-β-actin, anti-caspase-3, anti-NF-κB, anti-survivin, and anti-cleaved PARP, were purchased from Santa Cruz Biotechnology (USA). Rabbit polyclonal antibodies, anti-ERK1/2, anti-phopho-ERK1/2, anti-p38MAPK, anti-phospho-p38MAPK, anti-Akt, anti-phospho-Akt, anti-EGFR, anti-HER-2, and anti-mTOR were purchased from Genscript (USA). Pharmacological inhibitors SB202190 (p38MAPK inhibitor) and U-0126 (ERK inhibitor) were purchased from Cayman Chemical Company (USA). Lapatinib (EGFR inhibitor) was purchased from Biovision (USA). Stock solutions of compounds were prepared at appropriate concentrations in dimethyl sulfoxide (DMSO) and stored at −20°C in small aliquots.

MTT CYTOTOXICITY ASSAY

MDA-MB-231 cells were plated at a density of 2×10^4 cells/well in 96-well plates, allowed to attach overnight and treated with different concentrations of VA for 24 and 48 h. At the end of the treatment, 20 μl/well of MTT (5 mg/ml in phosphate-buffered saline—PBS) was added to each well and the plates were incubated for a further 3–4 h at 37°C in dark. Finally, the medium was removed and the purple-colored formazan precipitate was dissolved in optical grade DMSO (100 μl). The absorbance was read at 570 nm (reference wavelength 630 nm) in an ELISA plate reader (Bio-Rad, USA). The percentage of cytotoxicity was determined using the formula: Cytotoxicity (%) = (OD of control − OD of test/OD of control) × 100.

DETERMINATION OF MITOCHONDRIAL MEMBRANE POTENTIAL (ΔψM)

The changes in the mitochondrial membrane potential (Δψm) following VA treatment was analyzed using JC-1 (a lipophilic cationic fluorescent dye), capable of selectively entering the mitochondria. Under normal condition, JC-1 aggregates within the mitochondria and emits red fluorescence, but when the Δψm collapses during apoptosis, JC-1 leaks out into the cytosol as monomer and emits green fluorescence. The percentage of red to green fluorescence reflects the change in Δψm. Briefly, cells were cultured in coverslips placed in the wells of 6-well plates and incubated with VA for 24 and 48 h at 37°C. At the end of the treatment, cells were washed thrice in ice-cold PBS and then stained with JC-1 dye for 1 h in dark at 37°C. Mitochondrial membrane depolarization patterns of the cells were observed using fluorescent microscope (Carl Zeiss, Germany). For quantitative analysis, cells were seeded into 96-well plates and treated with IC_{50} concentrations of VA for 24 and 48 h. After treatment, the medium was removed and 100 μl of JC-1 (5 μg/ml) in each well was added to the cells and incubated for 30 min. Finally, the cells were washed twice with PBS and then quantitatively analyzed in a fluorescent microplate reader.

MEASUREMENT OF INTRACELLULAR REACTIVE OXYGEN SPECIES (ROS)

Intracellular ROS production was measured using 2,7-dichloro-fluorescein diacetate (H_2DCFDA; Sigma Aldrich). This dye is a stable non-polar compound that diffuses readily into cells and yields DCFH. Intracellular ROS, in the presence of peroxidase, changes DCFH to the highly fluorescent DCF. Thus, the fluorescence intensity is proportional to the amount of ROS produced by the cells. For ROS estimation, control and VA-treated cells were washed with HBSS and incubated in 1 ml of DCFH-DA at 37°C for 30 min. Stained cells were lysed in alkaline solution and centrifuged at 2,300*g* for 10 min. The supernatant, 0.2 ml, was transferred to a 96-well plate, and the fluorescence was measured using a fluorescent microplate reader. The values were expressed as percent of fluorescence intensity relative to control cells.

IMMUNOFLUORESCENCE

Bax translocation and EGFR expression in MDA-MB-231 cells were analyzed adopting immunofluorescent technique. Briefly, the cells were cultured in cover slips placed in the wells of 6-well plate and incubated with VA for 24 and 48 h. The cells were washed with ice-cold PBS, and fixed with 3.7% formaldehyde in PBS for 15 min. After washing thrice with PBS, the cells were permeabilized with

0.1% Triton X-100 in PBS at 37°C for 10 min. The cells were then blocked with bovine serum albumin (2% BSA) at room temperature for 1 h and, subsequently, incubated with Bax and EGFR antibodies (1:100) overnight at 4°C and with secondary antibodies conjugated with Alexa-fluor-488 for 1 h. The nuclei were stained with DAPI for 5 min after incubation with secondary antibody. Images were then captured with the fluorescent microscope (Carl Zeiss, Germany).

TUNEL DNA-END LABELING ASSAY

VA-induced apoptosis in MDA-MB-231 cells was detected using TUNEL (terminal deoxynucleotidyl transferase dUTP nick-end labeling) apoptosis detection kit (Genscript, USA). In brief, cells were fixed with 4% paraformaldehyde and permeabilized with 0.1% Triton X-100. TUNEL DNA-end labeling was performed with biotinylated nucleotide-dUTP in the presence of terminal deoxynucleotidyl transferase. Then horseradish peroxidase-labeled streptavidin (Streptavidin-HRP) was bound to the biotinylated nucleotides, which were detected using the peroxidase substrate, hydrogen peroxide, and 3,3′-diaminobenzidine (DAB) solution. Using this procedure, apoptotic nuclei were stained dark brown and observed in a light microscope (Olympus, Japan).

SDS–PAGE AND WESTERN BLOTTING

The cells were treated with VA for the specified time intervals and washed thrice with ice-cold PBS. The proteins were extracted with radioimmunoprecipitation assay (RIPA) lysis buffer (150 mM NaCl, 50 mM Tris, pH 8.0, 5 mM EDTA, 0.5% sodium deoxycholate, 0.1% SDS, 1.0% Nonidet P-40), supplemented with protease and phosphatase inhibitor cocktails (Sigma Aldrich), and quantified adopting Bradford method. After quantification, proteins (30 μg/lane) were subjected to 10–12% sodium dodecyl sulfate polyacrylamide gel electrophoresis (SDS–PAGE) to resolve the proteins, and then electrotransferred onto PVDF membrane. The membranes were incubated for 1–2 h at room temperature with blocking buffer (2% BSA in TBS), and then further incubated with the relevant primary antibodies overnight at 4°C. All primary antibodies were used at dilutions recommended by the manufacturer. After washing, membranes were incubated with the secondary antibody (anti-mouse or anti-rabbit IgG), alkaline phosphatase (ALP) conjugated for 1–2 h and the reaction was visualized using a chromogenic substrate BCIP/NBT (Calbiochem, USA).

STATISTICAL ANALYSIS

All data were obtained from at least three independent experiments and the results are expressed as mean ± SD (standard deviation). Differences between control and treated groups were analyzed using one-way analysis of variance (ANOVA). Statistical significance was inferred at P values less than 0.05.

RESULTS

THE CYTOTOXIC POTENTIAL OF VA IN MDA-MB-231 BREAST CANCER CELLS

The cytotoxic potential of VA in MDA-MB-231 breast cancer cells was determined by MTT assay. As shown in Figure 1B, cells were treated with varying concentrations of VA (0.2–1.6 μM/ml) for 24 and 48 h. VA exhibited significant time- and dose-dependent cytotoxicity ($P < 0.05$) with IC_{50} concentrations of 0.82 ± 0.02 and 0.58 ± 0.01 μM/ml for 24 and 48 h treatment periods, respectively. In particular, cells exposed to the highest concentration (1.6 μM/ml) underwent remarkable decrease in cell viability. In all the subsequent experiments, unless otherwise stated, we treated the cells with VA at these IC_{50} concentrations.

VA-INDUCED CHANGES IN CANCER CELLS REFLECTING MORPHOLOGICAL FEATURES OF APOPTOSIS

To find if VA treatment of MDA-MB-231 cells would induce changes in the nucleus that reflect apoptosis, hoechst 33258 staining was performed. Hoechst 33258 is a fluorescent dye which stains both healthy and apoptotic cells; however, healthy cells will stain homogeneously, whereas apoptotic cells will stain nuclei brightly. After VA exposure, MDA-MB-231 cells showed obvious morphological changes such as cell shrinkage, compaction of nuclei, and condensation and fragmentation of chromatin. In many cells the nuclei were fragmented (Fig. 1C; upper panel). The control cells did not undergo these changes.

To further confirm the VA-induced apoptosis, TUNEL assay was performed. TUNEL is one of the most popular method for identifying apoptotic cells in situ by detecting DNA strand breaks, which is a hall mark of apoptosis. As seen in Figure 1C (lower panel), in several VA-treated cells the nuclei were brown-colored, indicating that cells were undergoing apoptosis. These results are consistent with DNA fragmentation, apoptotic body formation, chromatin condensation, and apoptosis following VA treatment in MDA-MB-231 cancer cells.

VA-INDUCED INTRACELLULAR ROS GENERATION POTENTIATES ΔψM LOSS AND APOPTOSIS IN MDA-MB-231 CELLS

To find if induction of apoptosis as above by VA is linked to ROS generation and loss of Δψm, we determined the levels of ROS generation and Δψm in VA-treated MDA-MB-231 cells. As shown in Figure 2A,B, a significant time- and dose- dependent increase in ROS generation and Δψm loss were observed in VA-treated cells. To further substantiate a role for ROS in VA-induced cytotoxicity, cells were pre-treated with 6.5 mM NAC (ROS scavenger) for 1 h and then incubated with VA at IC_{50} concentrations for 24 and 48 h. Interestingly, NAC co-treatment effectively reversed the VA-induced ROS generation (Fig. 2A) and Δψm loss (Figs. 2B and C), indicating elevation of ROS levels as a key biochemical event in VA-induced cancer cell death.

We then analyzed the molecular redistribution by immunostaining of active Bax (Fig. 2D). As expected, in control cells there was no active Bax staining, whereas VA treatment for 24 h induced Bax activation, resulting in punctate Bax staining in cells. Along with the Δψm loss, VA treatment induced the release of cytochrome c to the cytosol fraction in a dose-dependent manner (Fig. 3B). Additionally, downregulation of anti-apoptotic Bcl-2, upregulation of pro-apoptotic Bax and PARP cleavage were also observed in VA-treated cells (Fig. 3B). To further examine the role of ROS in the VA-induced events toward apoptosis in the breast cancer cells, NAC was used for blocking the VA-induced ROS generation and apoptosis. Pre-

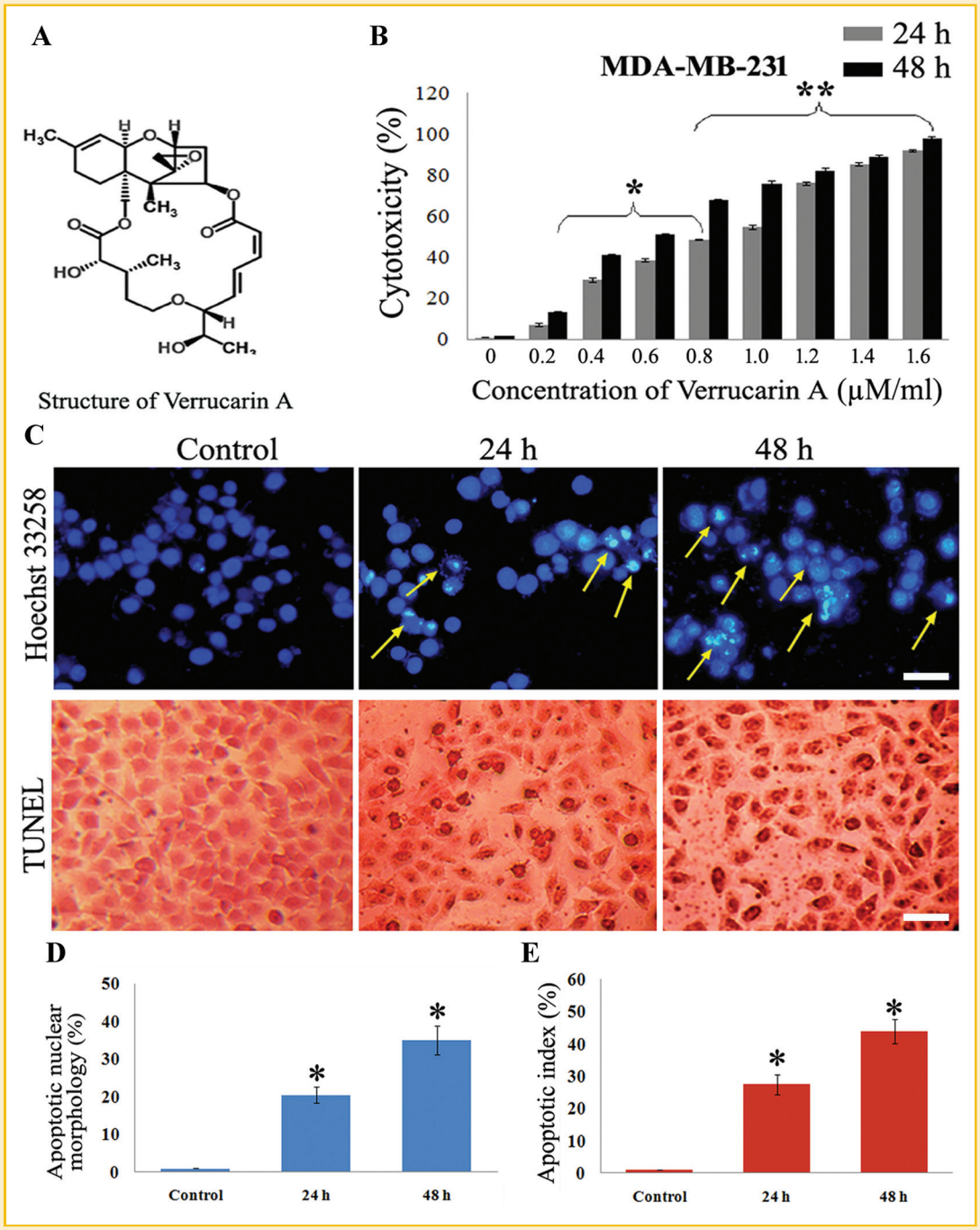

Fig. 1. Effect of VA on the growth and nuclear morphology of MDA-MB-231 cells. A: Structure and molecular formula of Verrucarin A. B: MDA-MB-231 cells were treated with varying concentrations of VA (0.2–1.6 μM/ml) for 24 and 48 h, and the cytotoxic potential of VA was determined by MTT assay. C: Upper panel—apoptotic nuclear morphology was analyzed by hoechst 33258 fluorescent staining. Arrows point to cells undergoing chromatin condensation and nuclear fragmentation. Scale bar 50 μm (_). C: Lower panel—to determine the apoptotic DNA damage, TUNEL assay was performed in cells as described in the Materials and Methods Section. VA-treated cells exhibited significant apoptotic DNA damage (indicated by the presence of dark brown color) whereas the control/untreated cells did not show DNA damage. Scale bar 50 μm (_). D: Bar chart showing the percentage of apoptotic nuclear morphological changes in control and VA-treated cells. E: Bar represents the TUNEL-positive cells in untreated and VA-treated cells. The apoptotic index of the VA treatment group was significantly higher than that of the control cells. Data are mean ± SD of three independent experiments. A significant difference between VA-treated and control cells indicated by $P < 0.05$(*) and $P < 0.01$(*).

treatment with NAC significantly inhibited the VA-induced cytotoxicity, cytochrome *c* release, Bcl-2 downregulation, Bax upregulation, and PARP cleavage (Fig. 3). Together, these results clearly indicate a role for ROS in VA-induced mitochondrial apoptosis. The results in Figures 1–3, suggest that VA causes cancer cell death through ROS-induced mitochondria-mediated pathway, which involves release of cytochrome *c* from mitochondria into the cytosol.

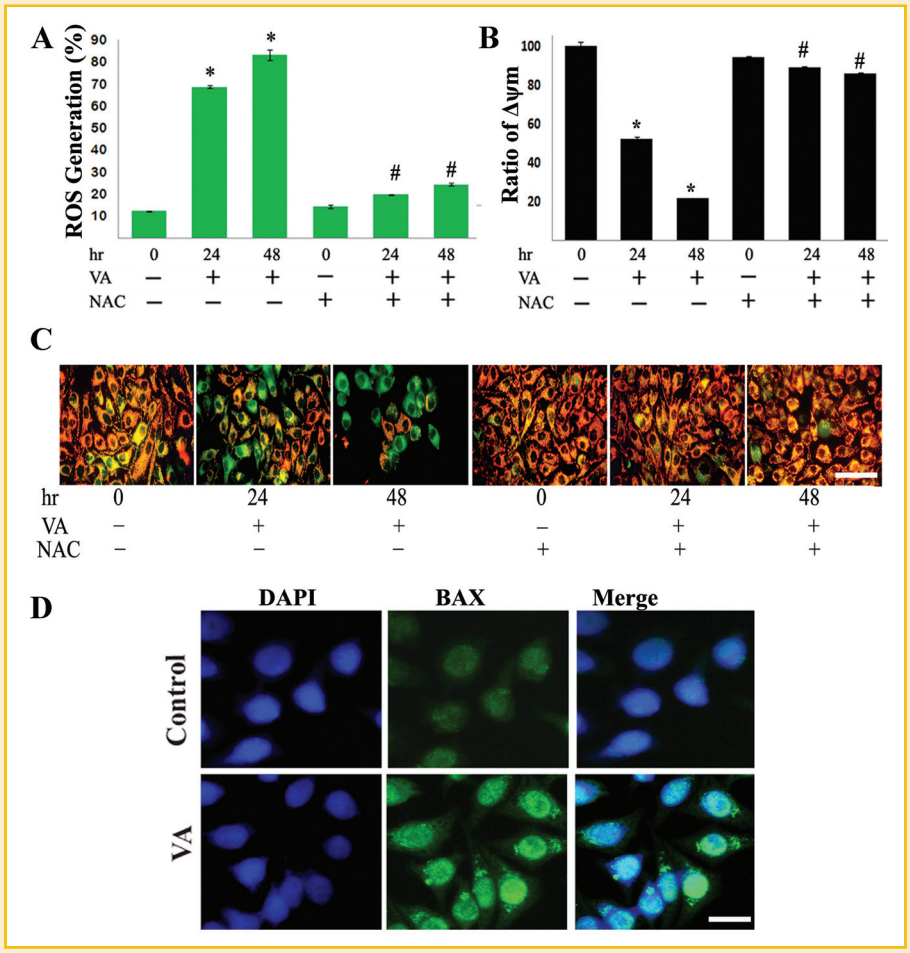

Fig. 2. Effect of VA on ROS generation and mitochondrial membrane potential ($\Delta\psi m$) in MDA-MB-231 cells. A: Cells were treated with VA at IC_{50} concentrations, 0.82 and 0.58 μM for 24 and 48 h, respectively, in the presence or absence of NAC. After treatment, cellular ROS levels were determined by using DCF-DA fluorescent dye in a fluorescent microplate reader. B: Mitochondrial membrane potential ($\Delta\psi m$) loss in VA-treated cells, determined by JC-1 fluorescent probe as described in the Materials and Methods Section. Data are mean ± SD of three independent experiments. $^{*}P < 0.05$ indicates significant difference between control and VA-treated cells. $^{\#}P < 0.05$ indicates significant difference between VA alone and co-treatment with NAC. C: Fluorescent photomicrographs show cells with reflections of mitochondrial membrane depolarization (loss of red fluorescence) after 24 and 48 h treatment with VA. Scale bar 50 μm (_). D: Immunostaining was performed to analyze the pro-apoptotic Bax protein translocation with an antibody specific for Bax (green fluorescence) and counterstaining with DAPI (blue fluorescence) to visualize the Bax expression and nuclear morphology. Scale bar 20 μm (_).

VA-INDUCED APOPTOSIS IN MDA-MB-231 CELLS INVOLVES ROS-MEDIATED p38MAPK ACTIVATION AND ERK1/2 INACTIVATION

MAPKs are serine threonine kinases, which are major information transducers from the cell membrane to the nucleus, and regulate cell survival/death. MAPKs also play crucial roles in a variety of chemotherapeutic agents-induced apoptotic signaling [Cowan and Storey, 2003]. To elucidate the putative signaling mechanism involved in VA-induced apoptosis, the effect of VA treatment on p38MAPK and ERK1/2 protein expression and phosphorylation were examined adopting Western blotting. As shown in Figure 4A, VA treatment significantly increased the phosphorylation levels of p38MAPK, while ERK1/2 phosphorylation level was significantly reduced. To confirm the mechanism by which ROS accumulation would increase the levels of p38MAPK activation, we pre-treated the cells with antioxidant NAC and then incubated with VA. The results showed that the activation of p38MAPK was effectively attenuated by NAC, which indicated that ROS plays a key role in VA-induced p38MAPK activation (Fig. 4A). To further elucidate the link between VA-induced apoptotic cell death and p38MAPK activation, the cells were pre-treated with 10 μM SB202190 (a potent p38MAPK inhibitor) for 1 h and then incubated with VA. It was found that VA-induced activation of p38MAPK was remarkably inhibited by SB202190 (Fig. 4C). Moreover, the p38MAPK inhibitor effectively attenuated the VA-induced cytotoxicity (Fig. 5A), upregulation of Bax, and downregulation of Bcl-2 and survivin, release of cytochrome *c* and cleavage of PARP in MDA-MB-231 cells (Fig. 5B). On the other hand, ERK1/2 activation was also inhibited by VA treatment (Fig. 4A). So, we assessed the contribution of ERK1/2 inhibition to VA-induced cytotoxicity and apoptosis. As shown in Figure 4C, pre-treatment of cells with 25 μM of U-0126 (specific ERK1/2 inhibitor) could effectively decrease the phosphorylation of ERK1/2 and increase the VA-induced PARP cleavage, Bax upregulation, and cytotoxicity (Fig. 5A).

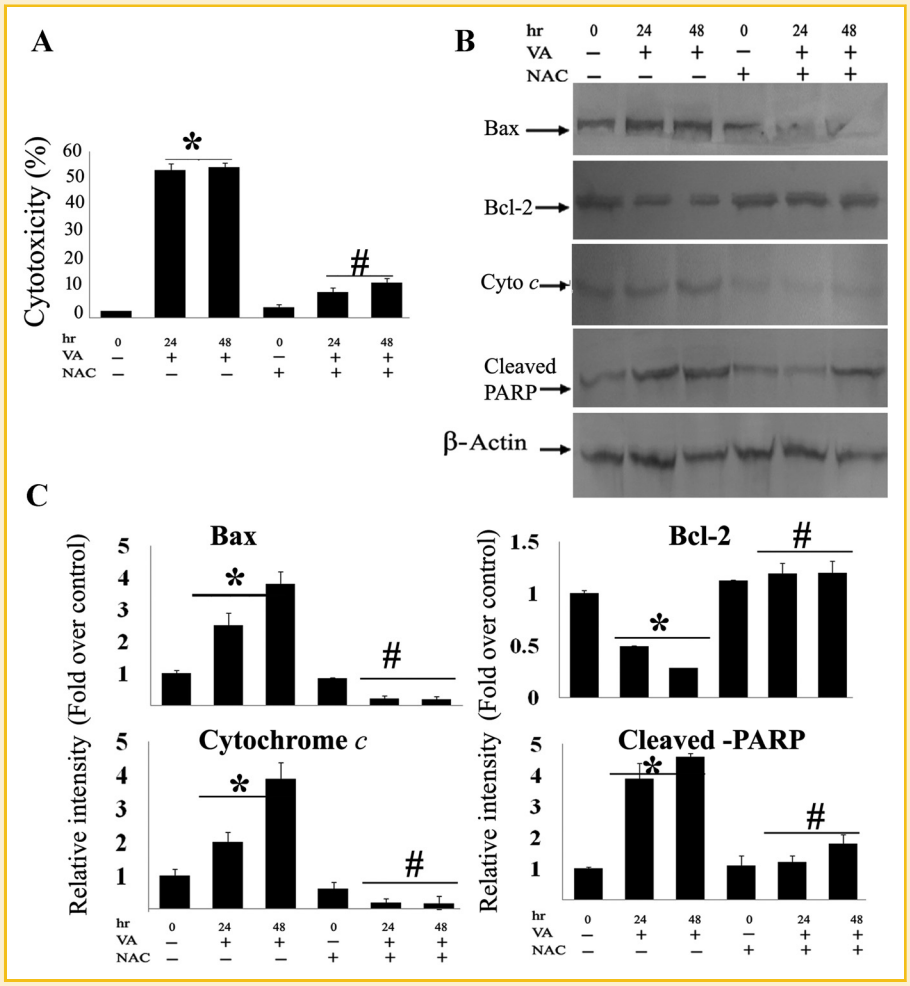

Fig. 3. VA-induces ROS-dependent apoptosis in MDA-MB-231 cells. Cells were pre-treated with 6.5 mM NAC (*n*-acetyl cysteine) and exposed to VA at IC_{50} concentrations, 0.82 and 0.58 μM for 24 and 48 h, respectively. A: NAC pre-treatment inhibits VA-induced cytotoxicity in MDA-MB-231 cells, analyzed by MTT assay. B: Western blotting analysis showing Bax upregulation, Bcl-2 downregulation, cytochrome *c* release, and PARP cleavage in VA-treated cells, whereas NAC pre-treatment significantly inhibited the VA-induced apoptotic signals. C: Bar diagram represents relative protein expression levels in control and treated cells. Data are mean ± SD of three independent experiments. $^{*}P < 0.05$ indicates significant difference between control and VA-treated cells. $^{\#}P < 0.05$ indicates significant difference between VA alone and co-treatment with NAC.

INHIBITION OF EGFR ACTIVATION AND ITS DOWNSTREAM SIGNAL-TRANSDUCTION MOLECULES CONTRIBUTION TO VA-INDUCED APOPTOSIS

To further elucidate the mechanisms underlying the VA-induced cytotoxicity, the relevant over-expressed signal transducers were examined adopting Western blotting technique. In MDA-MB-231 cells, EGFR and HER-2 are aberrantly over-expressed and well associated with each other, compared to normal cells. To analyze the expression of EGFR, immunostaining was performed in cells treated with VA. The results showed that VA treatment of MDA-MB-231 cells for 24 h decreased the expression of EGFR (Fig. 6A). VA produced a time- and dose-dependent suppression of the level of EGFR and HER-2 protein expression (Fig. 6B). Consequently, the phosphorylation and activation of downstream kinases such as Akt and ERK1/2 were also downregulated by treatment with VA. It is known that ERK1/2 and Akt promote cell proliferation and survival via modulating several downstream signaling molecules including mammalian target of rapamycin (mTOR), and nuclear factor-κB (NF-κB). Among them, mTOR regulates protein translation and thereby enhances cell growth, proliferation, and survival. To examine the effect of VA on activation of Akt-mediated signaling, the expression level of the mTOR was evaluated. As shown in Figure 4A, VA treatment suppressed the expression of phosphorylated Akt, which in turn caused downregulation of the expression of mTOR (Fig. 6B). Moreover, VA strongly suppressed the expression of NF-κB in MDA-MB-231 cells (Fig. 6B). Next, we assessed the functional role of ROS in VA-induced EGFR inhibition and apoptosis. As shown in Figure 6B, pre-treatment of cells with 6.5 μM of NAC (specific ROS scavenger) could effectively increase the phosphorylation of EGFR and HER-2. Moreover, NAC pre-treatment significantly reversed the VA-induced downregulation of mTOR, and NF-κB protein expression, indicating that ROS elevation suppresses EGFR activation and its downstream signal transduction molecule following VA exposure.

Next, we assessed the importance of EGFR inhibition on VA-induced cytotoxicity, and apoptosis. As shown in Figure 7B,

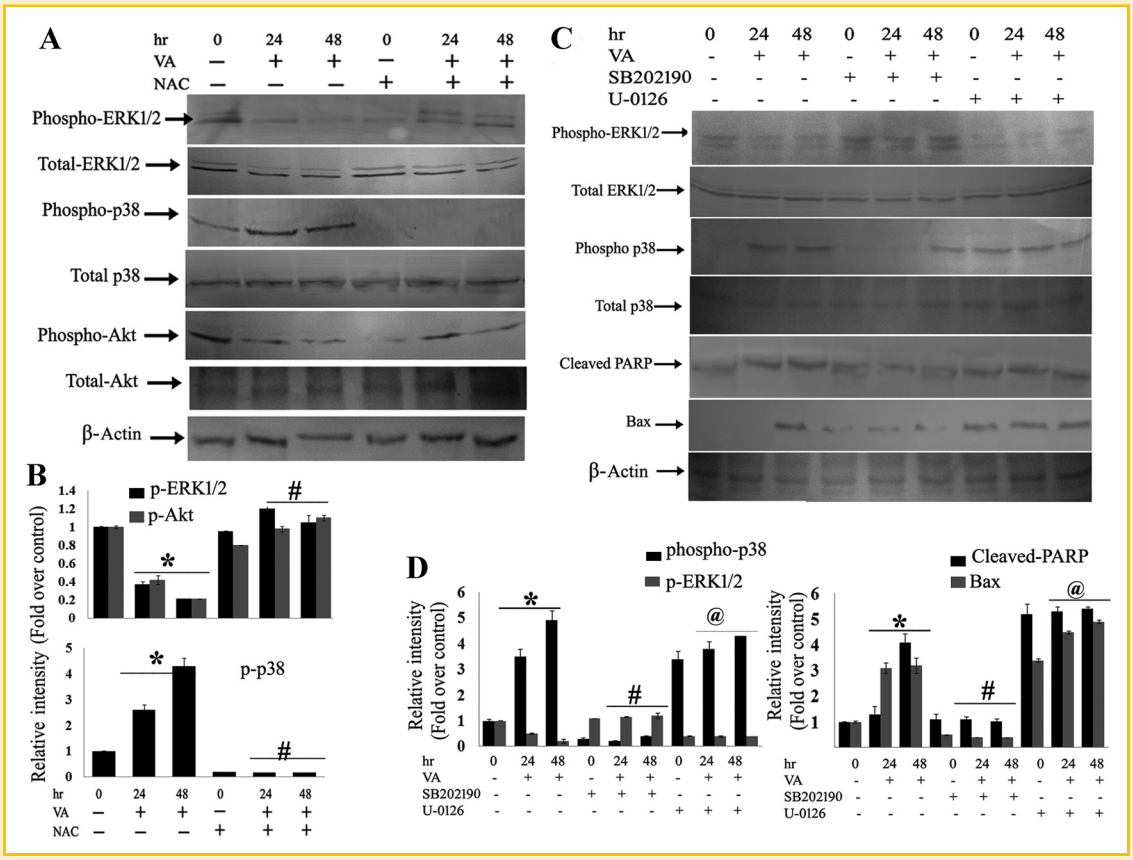

Fig. 4. ROS-dependent MAPK/Akt signal transduction pathways are associated with VA-induced apoptosis of MDA-MB-231 cells. A: Cells were treated with either NAC (ROS scavenger) or VA alone and in combination for 24 and 48 h. Equal amounts of proteins were separated by sodium dodecyl sulfate–polyacrylamide gel electrophoresis and the levels of total ERK1/2, p38MAPK, Akt and their phosphorylated forms were detected by Western blotting. B: Bar diagram represents relative protein expression levels in control and treated cells. Data are presented as mean ± SD of three independent experiments. $^{*}P < 0.05$ indicates significant difference between control and VA-treated cells. $^{\#}P < 0.05$ indicates significant difference between VA alone and co-treatment with NAC. C: MDA-MB-231 cells were treated with SB202190 (p38MAPK inhibitor), U0126 (ERK1/2 inhibitor) or VA alone and in combination, for 24 and 48 h. Then, the levels of total ERK1/2, phospho-ERK1/2, total-p38, phospho-p38, Bax, and cleaved-PARP proteins were detected by Western blotting. D: Bar diagram represents relative protein expression levels of phospho-p38MAPK, p-ERK1/2, Bax, and PARP in control and treated cells. Data are presented as mean ± SD of three independent experiments. $^{*}P < 0.05$ indicates significant difference between control and VA alone. $^{\#}P < 0.05$ indicates significant difference between VA alone and SB202190 + VA-treated cells at 24 and 48 h. $^{@}P < 0.05$ indicates significant difference between VA alone and U-0126 + VA-treated cells at 24 and 48 h, respectively.

co-treatment of cells with lapatinib (specific EGFR inhibitor) could effectively decrease the phosphorylation of EGFR, ERK1/2, Akt, and Bcl-2 protein expression. As expected, lapatinib co-treatment increased the VA-induced cytotoxicity (Fig. 7A), PARP cleavage, caspase-3 activation, and Bax protein upregulation (Fig. 7B). These results demonstrated that VA engages EGFR inhibition to induce the MAPK signal activation cascade, which involves caspase activation, to induce apoptosis.

DISCUSSION

Apoptosis is the most desired end point in the case of drug discovery for cancer and cancer therapy. The central finding of the present study is that VA induces apoptosis in MDA-MB-231 breast cancer cells by inducing ROS generation followed by mitochondria-dependent signaling pathway. Classical apoptotic cell death is an ordered and orchestrated cellular process for the elimination of unwanted cells including, cancer cells without causing inflammation. Apoptotic cells are characterized by a series of morphological alterations such as shrinkage of the cells and the nuclei, loss of adhesion to adjacent cells, membrane blebbing, DNA fragmentation, and chromatin condensation [Chen et al., 2010]. In this study, we first demonstrated that cells treated with VA exhibited characteristic apoptotic morphology, that is, cellular shrinkage, cytoplasmic blebbing, impaction of nuclei, DNA fragmentation, and condensation of chromatin.

Mitochondria play a crucial role in the apoptotic cell death induced by anti-cancer agents. The mitochondria-mediated cell death pathway is also referred as the intrinsic apoptotic pathway, and it plays a central role in apoptosis induced by the caspase-signaling cascade activation [Son et al., 2010]. Apoptosis signal can induce $\Delta\psi m$ loss and cytochrome *c* efflux from the mitochondria to the cytosol. In the cytosol, cytochrome *c* activates caspase-3, after which specific substrates of caspase-3, such as PARP, are cleaved,

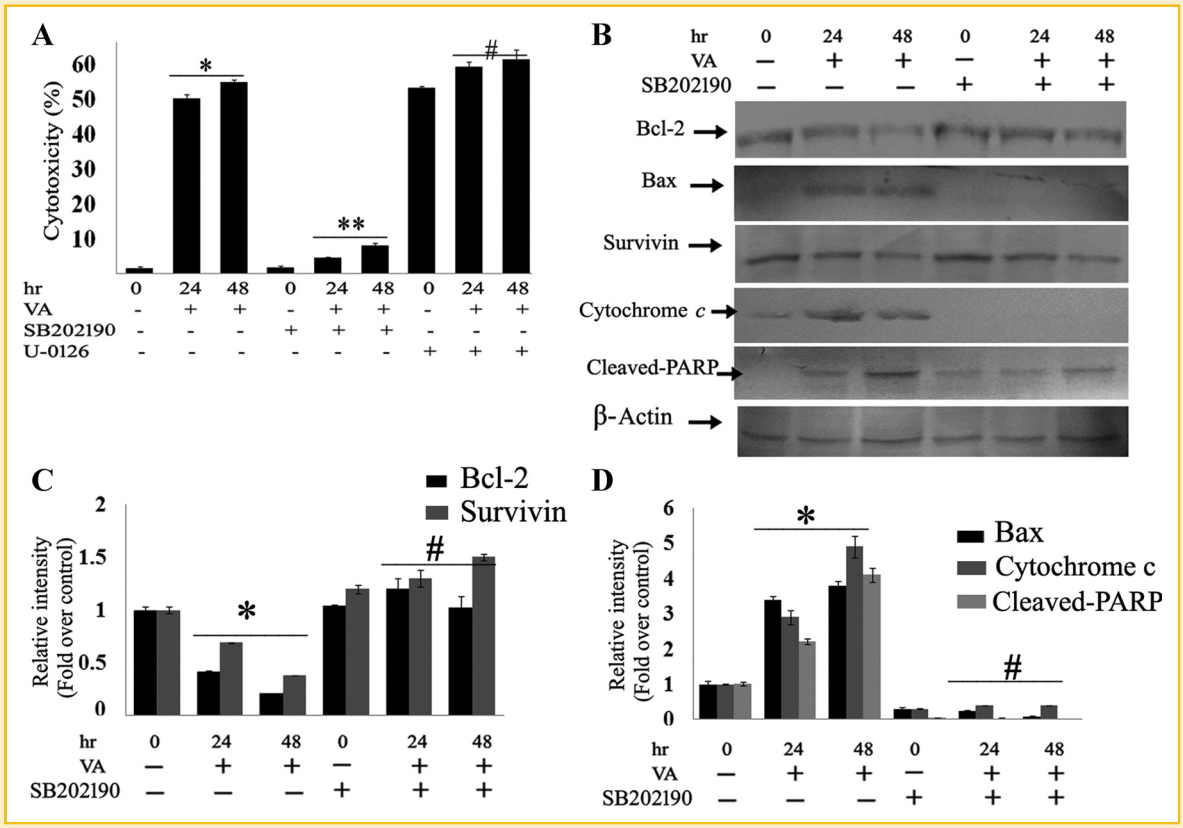

Fig. 5. VA-induces apoptosis through p38MAPK-activation in MDA-MB-231 cells. Cells were treated with either SB202190 (p38MAPK inhibitor) or VA alone and in combination, for 24 and 48 h. A: Then, MTT assay was performed to determine the cytotoxicity, and (B) Bcl-2, Bax, survivin, cytochrome c, and cleaved-PARP protein expressions were detected by Western blotting. C,D: Bar diagram represents relative protein expression levels in control and treated cells. Data are presented as mean ± SD of three independent experiments. $^{*}P < 0.05$ as compared with control. $^{\#}P < 0.05$ as compared with VA alone.

eventually leading to apoptosis. Bcl-2 family members are major regulators of cytochrome *c* release from the mitochondria, and they can change their conformations by forming mitochondrial permeability transition pores in the outer mitochondrial membrane to allow cytochrome *c* release into the cytosol.

Over-expression of anti-apoptotic Bcl-2 protein is known to protect cancer cells from apoptosis and to promote cell survival, its expression being correlated with the p53 status in the cells. On the contrary, over-expression of pro-apoptotic Bax accelerates apoptotic cell death. Bax forms oligomers in cytosol, which after being translocated to the mitochondrial membrane increases its permeability and induces the release of cytochrome *c* into cytosol. The cytosolic cytochrome *c* then forms a protein complex known as apoptosome, leading to the activation of caspase-9, which in turn cleaves and activates the effector caspases, such as caspases-7, and -3, and leads to PARP cleavage. Therefore, the Bax/Bcl-2 ratio plays a crucial role in cancer cell apoptosis induced by chemotherapeutic agents [Yip and Reed, 2008]. Our results showed that the expression of anti-apoptotic Bcl-2 dose-dependently decreased, whereas the expression of pro-apoptotic Bax dose-dependently increased. Caspases, a family of cysteine proteases, are activated during the execution phase of the apoptotic process. Once activated, these upstream caspases activate downstream caspases, leading to apoptosis. To determine whether VA-induced apoptosis of MDA-MB-231 cells was mediated via caspase cascade, the activation of caspases was detected by Western blotting. As shown, VA caused proteolytic cleavage of procaspase-3 in MDA-MB-231 cells in a time- and dose-dependent fashion. These results clearly indicated that the cytotoxic potential of VA against human breast cancer cell line MDA-MB-231 is associated with induction of mitochondria-dependent apoptosis.

Many anti-cancer agents, synthetic as well as natural, bring about antitumor activity through ROS-dependent apoptotic signaling. Elevated cellular ROS levels leads to the loss of mitochondrial membrane potential, which causes cytochrome *c* to leak out from the mitochondria in to the cytosol and ultimately triggers caspase-3 activation. Caspase-3 activation subsequently leads to DNA breakage, nuclear chromatin condensation, and apoptosis. VA treatment caused time- and dose-dependent elevation in the cellular ROS production, and the VA-induced apoptotic signals (cytochrome *c* release, Bcl-2 downregulation, Bax upregulation, and PARP cleavage) were significantly attenuated by the ROS-scavenger NAC. These results indicated that the VA-induced apoptotic cell death in human breast cancer cells is initiated by ROS generation.

It has been reported that MAPKs are involved in the mechanisms underlying apoptotic cell death. ERK1/2 behaves mainly as a

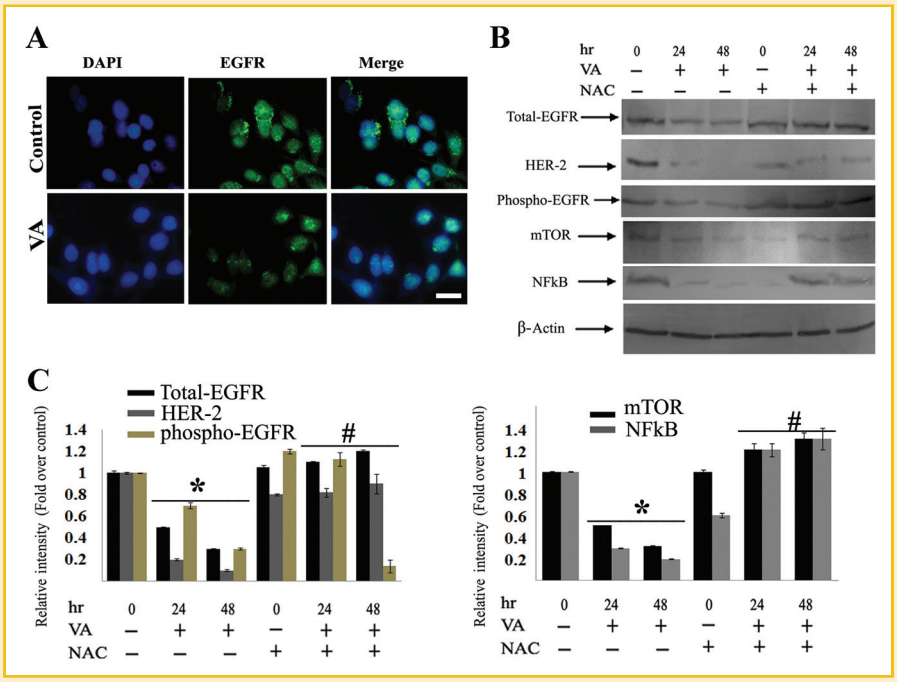

Fig. 6. Involvement of EGFR signaling pathway in VA-induced apoptosis of MDA-MB-231 cancer cells. A: Cells were treated with VA (IC_{50}) and immunostaining was performed to analyze the EGFR protein expression with an antibody specific for EGF receptor (green fluorescence) and counterstaining with DAPI (blue fluorescence) to visualize the EGFR expression and nuclear morphology. B: Cells were treated with either NAC (ROS scavenger) or VA alone and in combination, for 24 and 48 h. Equal amounts of proteins were separated by sodium dodecyl sulfate–polyacrylamide gel electrophoresis and the protein expressions of total-EGFR, phospho-EGFR, HER-2, mTOR, and NF-κB were detected by Western blotting. C: Bar diagram represents relative protein expression levels in control and treated cells. Data are presented as mean ± SD of three independent experiments. $^{*}P < 0.05$ as compared with control. $^{\#}P < 0.05$ as compared with VA alone.

mitogen-activated proliferation/differentiation factor, whereas JNK and p38MAPK are mainly stress-activated proteins related to apoptotic cell death [Tamura et al., 2002]. Therefore, the balance between ERK and JNK/p38 activation is responsible for cells′ fate, that is, whether cells undergo differentiation, proliferation, or apoptosis [Cowan and Storey, 2003]. Our result demonstrated that VA treatment enhanced p38MAPK activation in MDA-MB-231 cells, indicating that the apoptotic effect of VA may be associated with activation of stress-induced p38MAPK. In addition, co-treatment with NAC (ROS-scavenger) and SB202190 (p38MAPK inhibitor) significantly abrogated the VA-induced p38MAPK activation and apoptotic signals. On the other hand, ERK1/2 inhibition by U-0126 significantly enhanced the VA-induced apoptotic signals. These results indicated that ROS-induced p38MAPK activation and ERK inactivation play a crucial role in VA-induced apoptosis.

EGFR, a proto-oncogene, plays a critical role in tumorigenesis by modulating proliferation, differentiation, and DNA damage response [Rodemann et al., 2007]. In general, EGFR and HER-2, are the major targets of RTK ErbB family, which is upregulated in triple-negative breast cancer cells including MDA-MB-231 cells [Zandi et al., 2007]. It is well known that stimulation of EGFR results in activation of Akt and ERK1/2, two major signaling pathways for cell survival and cellular proliferation [Lawlor and Alessi, 2001].

Akt is an anti-apoptotic kinase that promotes cell survival and blocks apoptosis. EGFR-Akt activation regulates mTOR activity which is important for cell proliferation [Galbaugh et al., 2006]. A large body of evidence suggests that mTOR is greatly associated with carcinogenesis, and mTOR signaling pathway is dysregulated in premalignant or early malignant human tissues. Besides, activated Akt can also promote the transcriptional activity of NF-κB, a nuclear transcription factor, which plays a crucial role in inflammation, cell proliferation, apoptosis, invasion, angiogenesis, metastasis, chemoresistance, and radioresistance. Previous studies have demonstrated that targeting signaling pathways mediated by either EGFR or NF-κB, directly or indirectly, represents a possible tactic to improve therapeutic outcome in cancer patients [Aggarwal, 2004]. Our study identified that VA was able to inhibit EGFR, ERK1/2, and Akt phosphorylation in MDA-MB-231 cells, which, in turn, altered the expression of mTOR and NF-κB, thus inhibiting MDA-MB-231 cell growth. However, our results showed that in MDA-MB-231 cells, inhibition of EGFR by lapatinib (a potent EGFR inhibitor) further enhanced VA-induced procaspase-3 proteolysis, Bcl-2 downregulation, and Bax upregulation at the concentration that blocks the phosphorylation of EGFR. Thus, a much more complex mechanism for inhibition of EGFR by VA appears to be involved and will be examined in further studies.

Despite the fact that many anti-cancer agents are practiced for breast cancer, metastatic triple-negative breast cancer remains a major threat to women′s health worldwide, particularly because these cancer cells eventually become resistant to apoptosis [Lee and Swain, 2005]. For example, cisplatin and doxorubicin are used in breast cancer treatment and both have been shown to induce

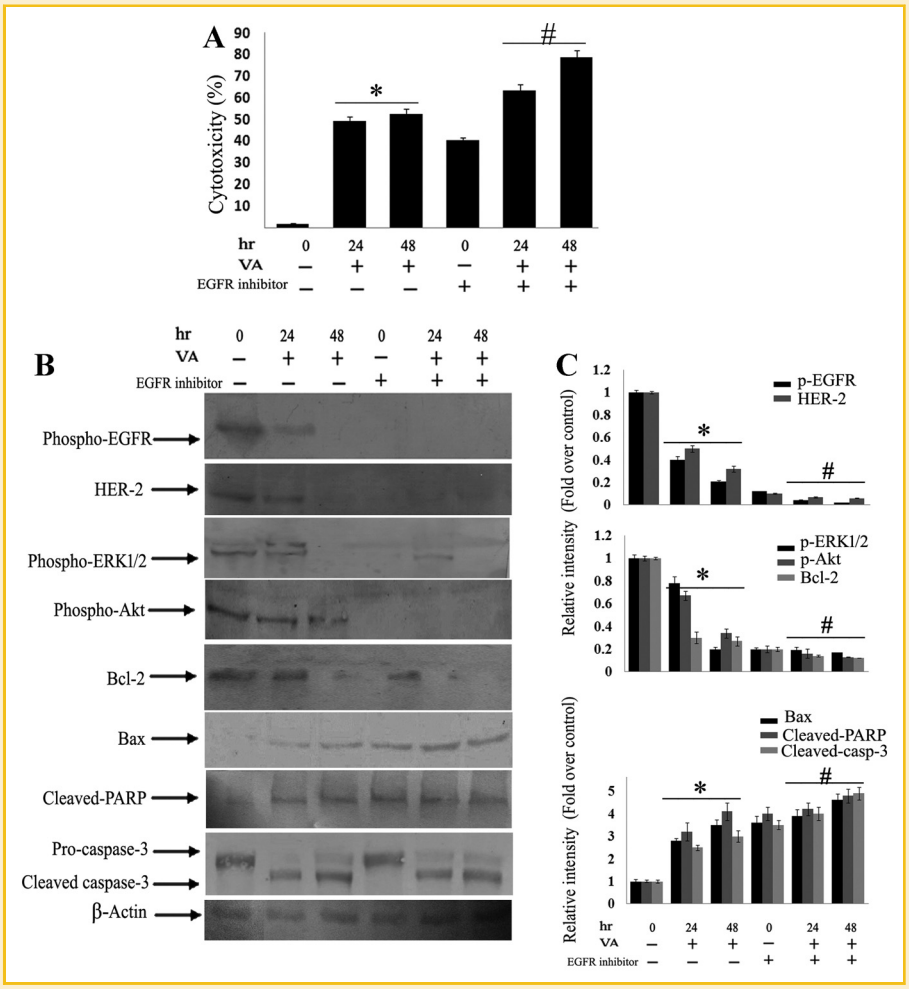

Fig. 7. Inhibition of EGFR activation promotes apoptosis in MDA-MB-231 cells. A: Cells were treated with either lapatinib (EGFR inhibitor) or VA alone, and in combination, for 24 and 48 h. Then, cytotoxicity was determined by the MTT assay, and (B) the protein expression of phospho-EGFR, HER-2, phospho-ERK1/2, phospho-Akt, Bcl-2, Bax, cleaved-PARP, and caspase-3 were analysed by Western blotting. β-actin was used as internal control. C: Bar diagram represents relative protein expression levels in control and treated cells. Data are presented as mean ± SD of three independent experiments. $^{*}P < 0.05$ as compared with control. $^{\#}P < 0.05$ as compared with VA alone.

apoptosis in MDA-MB-231 breast cancer cells, at a dose around 90–100 μM/ml for cisplatin, and about 2–5 μM/ml for doxorubicin [Tassone et al., 2003; Aroui et al., 2009; Nestal de Moraes et al., 2013], but the cells develop resistance in cause of time [Real et al., 2002]. The human breast cancer cell line MDA-MB-231 is a highly invasive, basal-like phenotype and is usually considered as an apoptosis-resistant cell line. In our study, data are consistent with these findings, showing an increase in apoptotic cells and reduction in viability, following treatment with very low doses of VA (0.6–1 μM/ml), also pointing to an advantage that VA treatment would potentially circumvent the development of resistance to apoptosis. Activation of EGFR/MAPK/Akt protein kinases correlates with proliferation, malignancy, and resistance to apoptosis in metastatic breast cancer cells [Lawlor and Alessi, 2001; Galbaugh et al., 2006; Rodemann et al., 2007; Zandi et al., 2007]. Therefore, novel-targeted therapeutic strategies are desired to circumvent the resistance to apoptosis in breast cancer cells. For instance, lapatinib, an EGFR inhibitor, has been shown to surmount apoptosis resistance in metastatic breast cancer cells [Nahta et al., 2007]. Here, we present the evidence that the inhibitory effect of VA in MDA-MB-231 breast cancer cells is brought about by antagonizing and inhibiting the activation of EGFR/MAPK/Akt protein kinases. Therefore, we suggest that VA and EGFR/MAPK/Akt protein kinase inhibitors in combination, may be an appropriate therapeutic strategy to overcome apoptosis resistance in metastatic breast cancer cells, and this will be examined in our future studies.

In summary, we report that VA treatment induces apoptosis in human breast cancer cell line MDA-MB-231 via ROS generation and activation of the signaling kinase p38MAPK. In addition, VA inhibits the phosphorylation of EGFR, which is also involved in the inhibition of ERK1/2 and Akt activation, leading to apoptosis signal activation in MDA-MB-231 cells. NAC (ROS scavenger) and inhibitor of p38MAPK (SB202190) substantially inhibited the cytotoxic effect of VA, suggesting an important role for ROS generation and p38MAPK activation in VA-induced apoptosis. Future studies will be needed to further substantiate the importance of the mechanisms elucidated

herein, and to develop targeted cancer therapies on the basis of our findings.

ACKNOWLEDGMENTS

This study was supported by University Grants Commission, India, under the Special Assistance Programme (UGC–SAP)-Research Fellowship for Meritorious Students in Science (RFMS).

REFERENCES

Aggarwal BB. 2004. Nuclear factor-kappa B: The enemy within. Cancer Cell 6:203–208.

Andersen B, Nielsen KF, Jarvis BB. 2002. Characterization of *Stachybotrys* from water-damaged buildings based on morphology, growth, and metabolite production. Mycologia 94:392–403.

Aroui S, Brahim S, De Waard M, Bréard J, Kenani A. 2009. Efficient induction of apoptosis by doxorubicin coupled to cell-penetrating peptides compared to unconjugated doxorubicin in the human breast cancer cell line MDA-MB-231. Cancer Lett 285:28–38.

Chen YW, Huang CF, Yang CY, Yen CC, Tsai KS, Liu SH. 2010. Inorganic mercury causes pancreatic beta-cell death via the oxidative stress induced apoptotic and necrotic pathways. Toxicol Appl Pharmacol 243:323–331.

Cowan KJ, Storey KB. 2003. Mitogen-activated protein kinases: new signalling pathways functioning in cellular responses to environmental stress. J Exp Biol 206:1107–1115.

Galbaugh T, Cerrito MG, Jose CC, Cutler ML. 2006. EGF-induced activation of Akt results in mTOR-dependent p70S6 kinase phosphorylation and inhibition of HC11 cell lactogenic differentiation. BMC Cell Biol 7:34.

Kamata H, Hirata H. 1999. Redox regulation of cellular signalling. Cell Signal 11:1–14.

Lawlor MA, Alessi DR. 2001. PKB/Akt: A key mediator of cell proliferation, survival and insulin responses? J Cell Sci 114:2903–2910.

Lee JJ, Swain SM. 2005. Development of novel chemotherapeutic agents to evade the mechanisms of multidrug resistance (MDR). Semin Oncol 32:22–26.

Looyenga BD, Hutchings D, Cherni I, Kingsley C, Weiss GJ, MacKeigan JP. 2012. STAT3 is activated by JAK2 independent of key oncogenic driver mutations in non-small cell lung carcinoma. PLoS One 7:e30820.

Nahta R, Yuan LX, Du Y, Esteva FJ. 2007. Lapatinib induces apoptosis in trastuzumab-resistant breast cancer cells: Effects on insulin-like growth factor I signaling. Mol Cancer Ther 6(2):667–674.

Nestal de Moraes G, Vasconcelos FC, Delbue D, Mognol GP, Sternberg C, Viola JP, Maia RC. 2013. Doxorubicin induces cell death in breast cancer cells regardless of survivin and XIAP expression levels. Eur J Cell Biol 92:247–256.

Oda T, Namikoshi M, Akano K, Kobayashi H, Honma Y, Kasahara T. 2005. Verrucarin A inhibition of MAP kinase activation in a PMA-stimulated promyelocytic leukemia cell line. Mar Drugs 3:64–73.

Palanivel K, Kanimozhi V, Kadalmani B, Akbarsha MA. 2013. Verrucarin A, a protein synthesis inhibitor, induces growth inhibition and apoptosis in breast cancer cell lines MDA-MB-231 and T47D. Biotechnol Lett 35:1395–1403.

Peddi PF, Ellis MJ, Ma C. 2012. Molecular basis of triple negative breast cancer and implications for therapy. Int J Breast Cancer 2012:217185.

Rao GN. 1996. Hydrogen peroxide induces complex formation of SHCGrb2-SOS with receptor tyrosine kinase and activates Ras and extracellular signal-regulated protein kinases group of mitogen-activated protein kinases. Oncogene 13:713–719.

Real PJ, Sierra A, De Juan A, Segovia JC, Lopez-Vega JM, Fernandez-Luna JL. 2002. Resistance to chemotherapy via Stat3-dependent overexpression of Bcl-2 in metastatic breast cancer cells. Oncogene 21:7611–7618.

Rodemann HP, Dittmann K, Toulany M. 2007. Radiation-induced EGFR signalling and control of DNA-damage repair. Int J Radiat Biol 83:781–791.

Selvendiran K, Bratasz A, Tong L, Ignarro LJ, Kuppusamy P. 2008. NCX-4016, a nitro derivative of aspirin, inhibits EGFR and STAT3 signaling and modulates Bcl–2 proteins in cisplatin-resistant human ovarian cancer cells and xenografts. Cell Cycle 7:81–88.

Son YO, Hitron JA, Wang X, Chang QS, Pan JJ, Zhang Z, et al. 2010. Cr (VI) induces mitochondrial-mediated and caspase-dependent apoptosis through reactive oxygen species-mediated p53 activation in JB6 Cl41 cells. Toxicol Appl Pharmacol 245:226–235.

Tamura S, Hanada M, Ohnishi M, Katsura K, Sasaki M, Kobayashi T. 2002. Regulation of stress-activated protein kinase signaling pathways by protein phosphatases. Eur J Biochem 269:1060–1066.

Tassone P, Tagliaferri P, Perricelli A, Blotta S, Quaresima B, Martelli ML, Goel A, Barbieri V, Costanzo F, Bol CR, Venuta S. 2003. BRCA1 expression modulates chemosensitivity of BRCA1-defective HCC1937 human breast cancer cells. Br J Cancer 88:1285–1291.

Yip KW, Reed JC. 2008. Bcl-2 family proteins and cancer. Oncogene 27:6398–6406.

Zandi R, Larsen AB, Andersen P, Stockhausen MT, Poulsen HS. 2007. Mechanisms for oncogenic activation of the epidermal growth factor receptor. Cell Signal 19:2013–2023.